Creating capillary networks within human engineered tissues: impact of adipocytes and their secretory products

Kim Aubin [#a,b], Caroline Vincent [#a,b], Maryse Proulx[a,b], Dominique Mayrand[a,b] and Julie Fradette*[a, b, c]

[a] Centre de recherche en organogénèse expérimentale de l'Université Laval / LOEX

[b] Division of Regenerative Medicine, CHU de Québec Research Centre

[c] Department of Surgery, Faculty of Medicine, Université Laval, Québec, QC, Canada

# Both authors contributed equally

[*] Corresponding author:

Julie Fradette, PhD

LOEX, Aile-R, Hôpital Enfant-Jésus

CRCHU de Québec

1401, 18e Rue

Québec, QC, G1J 1Z4

Tel: 1-418-990-8255 Ext. 1713

Fax: 1-418-990-8248

Julie.fradette@chg.ulaval.ca

www.loex.qc.ca

Running title: Impact of microenvironment on capillary networks *in vitro*

ABSTRACT

The development of tissue-engineered substitutes of substantial volume is closely associated with the need to ensure rapid vascularization upon grafting. Strategies promoting angiogenesis include the *in vitro* formation of capillary-like networks within engineered substitutes. We generated both connective and adipose tissues based on a cell sheet technology using human adipose-derived stromal cells. This study evaluates the morphology and extent of the capillary networks that developed upon seeding of human microvascular endothelial cell during tissue production. We posited that adipocyte presence/secretory products could modulate the resulting capillary network when compared to connective substitutes. Analyses including confocal imaging of CD31-labeled capillary-like networks indicated slight differences in their morphological appearance. However the total volume occupied by the networks as well as the frequency distribution of the structure's volumes were similar between connective and adipose tissues. Average diameter of the capillary structures tended to be 20% higher in reconstructed adipose tissues. Quantification of pro-angiogenic molecules in conditioned media showed greater amounts of leptin (15x), angiopoietin-1 (3.4x) and HGF (1.7x) secreted from adipose than connective tissues at the time of endothelial cell seeding. However, this difference was attenuated during the following coculture period in endothelial cell-containing media, correlating with the minor differences noted between the networks. Taken together, we developed a protocol allowing reconstruction of both connective and adipose tissues featuring well-developed capillary networks *in vitro*. We performed a detailed characterization of the network architecture within engineered tissues that is relevant for graft assessment before implantation as well as for *in vitro* screening of angiogenic modulators using 3D models.

Keywords: Adipose-derived stem/stromal cells, adipose substitute, tissue engineering, endothelial cells, capillary formation, confocal microscopy.

1. INTRODUCTION

Adipose tissue (AT) is endowed with great plasticity. Expansion and regression of fat depots occur throughout life. Such variations in adipose volume are generally accompanied by a concomitant adaptation of the local fat pad vascular supply [1-3]. AT features a well-defined vascular network comprising many capillaries surrounding lipid-filled adipocytes [4, 5]. This vasculature is central in mediating the metabolic roles of AT as an endocrine and paracrine organ. The numerous growth factors, hormones and pro-angiogenic factors that are produced by adipose tissue and collectively termed adipokines are now recognized as essential regulators of many biological processes including lipid metabolism, angiogenesis, reproduction and immunometabolism [6-9]. Secreted molecules from both mature adipocytes and from cell populations of the stromal-vascular fraction contribute to the adipose tissue secretome [10]. The stromal fraction contains various cell types *in vivo* including the subpopulation of cells featuring multipotent differentiation capabilities that be can extracted and amplified *in vitro* named ASCs (adipose-derived stromal/stem cells) [11]. The therapeutic effect of ASC-based cellular therapies was also reported to be mainly mediated by their trophic and paracrine functions [6, 12].

In situations necessitating soft tissue augmentation, autologous fat grafting is still the gold standard procedure. However, lipoinjections likely disrupt both adipocytes and the adipose graft vascular network, which might be contributing factors to the rather limited and variable long-term volume retention achieved by fat transfer methods in general [13, 14]. Consequently, the field of adipose tissue engineering has thrived in recent years. Various models are currently developed to help circumvent some of the actual limitations associated with fat grafting [15-17]. One of tissue engineering biggest challenges resides in the production of thick substitutes needing

to be quickly and adequately vascularized after grafting. That also holds true for adipose tissues reconstructed for regenerative medicine purposes. One strategy is to favor early inosculation of the graft to the host circulation, which requires the presence of a preformed capillary network *in vitro* [18]. This can be achieved by the incorporation of endothelial cells at different steps of tissue production [19, 20].

Using ASCs as building blocks for tissue engineering by the self-assembly approach, we have reconstructed natural and functional human tissues [21]. ASCs being particularly performant for extracellular matrix (ECM) deposition and cell-sheet formation, connective tissues can readily be reconstructed upon serum and ascorbic acid (AsA) stimulation in culture [22]. These human reconstructed connective tissues (hrCT) can find applications as such or as stromal compartments (dermis) upon which keratinocytes can be seeded for skin substitute production [23]. When combined with an adipogenic induction step during production, the resulting adipose tissues (hrAT) feature functional adipocytes embedded into native extracellular matrix, as assessed by their capacity to mediate β-adrenergic lipolysis and secrete various adipokines [21, 24].

In this study, we demonstrate that human microvascular endothelial cells (hMVEC) incorporation at specific steps during tissue production results in the spontaneous formation of capillary-like networks both in hrCT and hrAT. We tested the hypothesis that adipocytes and their potent secretory products could modulate the resulting capillary network when compared to connective substitutes produced from the same cell populations in absence of adipogenic stimulation. Our results indicate that under specific culture conditions, hMVEC self-organize to form microvascular networks without impacting on tissue thickness or adipocyte development. The resulting CD31-labeled networks imaged by confocal microscopy were well-developed and slight

variations in their morphology were associated with adipocyte presence. Bioactive molecules known to influence angiogenic processes were evaluated in conditioned media at various time-points during tissue production. Although the microenvironment seen by hMVEC was distinct in presence of adipocytes at the time of hMVEC seeding, this difference was attenuated during the following period in endothelial cell coculture media, therefore limiting the direct impact of adipocyte-derived factors. In combination with detailed imaging of capillary networks, these engineered tissues represent relevant adipose models for investigation of pro- and anti-angiogenic compounds in addition to their intended use in regenerative medicine.

2. MATERIAL and METHODS

2.1 Cell isolation and amplification

All protocols were approved by the Institutional review board of the CRCHU de Québec. Human ASCs (hASCs) were extracted using collagenase digestion of tissues obtained after lipoaspiration procedures (N=4 cell populations). Female donor's mean age was 38.3 ± 2.4 years and mean body mass index was 28.3 ± 0.93. hASCs were amplified in standard culture medium (DH) composed of 1:1 Dulbecco's modified Eagle's medium (DMEM): Ham's F12 medium (H) (Life Technologies, Burlington, ON, Canada) supplemented with 10% foetal calf serum (FCS) (HyClone, Logan, UT, United States) and antibiotics [100 U/ml penicillin (Sigma-Aldrich, Oakville, ON, Canada) and 25 µg/ml gentamicin (Schering-Plough Canada Inc./Merck, Scarborough, ON, Canada)] (Table 1). They were batch frozen at passage (P) 0 until being used for tissue reconstruction [21].

Human microvascular endothelial cells (hMVEC) were kindly provided by V. Moulin and S. Chabaud. Briefly, cells were extracted from the dermis of a 59 year-old female donor as described previously [20], with the modification that the skin biopsy was incubated overnight in thermolysin solution (Sigma) [25] instead of dispase. Thawed cells were plated at $1x10^4$ cells/cm^2 density on gelatin-coated culture dishes (BD Biosciences, Mississauga, ON, Canada) in endothelial cell media consisting of complete EGM™-2MV BulletKit™ (EGM2) media (Clonetics/Lonza, Walkersville, MD, USA) containing 5% foetal bovine serum (FBS) and antibiotics [100 U/ml penicillin (Sigma-Aldrich) and 25 µg/ml gentamicin (Schering-Plough Canada Inc./Merck) instead of the GA-1000 (Gentamicin, Amphotericin-B) provided by the manufacturer], amplified and used at P6 in microvascularized reconstructed tissues.

2.2 Production of human connective and adipose reconstructed tissues

For tissue reconstruction, hASCs were used at P3-5. After thawing, cells were seeded in DH media at $8x10^3$ cells/cm^2 into Nunc flasks (Thermo Fisher Scientific, Waltham, MA, USA) [26]. After expansion, hASCs were seeded onto Nunc 6-well plates for tissue production at a density of 1.56×10^4 cells/cm^2, in presence of 50 µg/ml (250 µM) AsA (Sigma-Aldrich) freshly prepared at each media change (every 2-3 days). After 7 days of culture, half of the plates were induced towards adipogenic differentiation for 3 days using a defined cocktail [100 nM insulin (Sigma), 0.2 nM T3 (Sigma), 1 µM dexamethasone (Sigma), 0.25 mM 3-isobutyl-1-methylxanthine (IBMX) (Sigma) and 1 µM rosiglitazone (Cayman Chemical/ Cedarlane, Burlington, ON, Canada)] in 3% FCS-containing medium, followed by culture in adipocyte maintenance media for the rest of the culture period [21, 26]. Mock-induced cells were cultured for 3 days in DH media with 3% FCS and 0.038% dimethyl sulfoxide (DMSO, diluent for IBMX and rosiglitazone), followed by culture in 10% FCS DH media until endothelial cell seeding (see Table 1).

After 21 days in culture and 14 days of adipogenic differentiation, hMVEC at a density of 2.08×10^4 cells/cm^2 were added to a subset of the cultures previously induced or not towards adipogenesis (Fig. 1). Culture was performed in a mixed coculture media for both adipocytes and hMVEC, namely a (1:1) ratio of EGM2 media (5% FBS) and DH adipocyte maintenance media (10% FCS), also supplemented with AsA (Table 1). Cell cultures onto which no hMVEC were added were also cultured into the mixed (1:1) EGM2: DH or adipogenic maintenance media for proper comparative purposes. At day 30 of culture (and day 23 of adipocyte differentiation), the

matrix secreted and organized by the cells formed a manipulatable cell sheet, containing or not adipocytes and/or hMVEC. Thicker tissues were then engineered by the superposition of 3 cell sheets (maintaining their initial orientation with hMVEC on top). These reconstructed tissues were further cultured for 12 days to favor cohesion between cell sheets before being analyzed at day 42 of culture. Therefore, hMVEC have been present in the engineered tissues for a total of 21 days. hMVEC seeding was also performed at earlier time-points during optimization, as indicated in Fig. 2G (after 3 and 7 days of adipogenic induction). Reference tissues were produced for the analysis of conditioned media. These adipose and connective tissues devoid of hMVEC were cultured in adipogenic or DH media only for similar culture periods (Table 1).

2.3 Histological analyses and measurements

Formalin-fixed paraffin embedded samples of the different tissues were analyzed after Masson's trichrome staining of 5 µm-thick sections. Pictures were acquired on a microscope Nikon Eclipse Ts100 equipped with a Nikon Coolpix 4500 camera (Nikon, Montreal, Qc). Thickness determination was performed on tissue cross-sections using the ImageJ 1.48 software (NIH, http://rsb.info.nih.gov/ij/). For each type of construct, 2-5 tissues from 4 different donors were evaluated. A minimum of 12 pictures per tissue were acquired and 3 measurements were taken per picture.

2.4 Quantification of adipose differentiation by Oil Red O staining

Oil Red O (ORO) staining and quantification of the cytoplasmic droplets of neutral lipids were performed on adipose and their control connective sheets after a typical 14-15 day period after adipogenic induction [21]. Induction of differentiation was performed at day 7 of culture while hMVEC seeding was performed either at day 10, 14 or 21 of culture. Results are expressed as the

mean ± SEM of the ORO values obtained for each cell population. ORO values represent the optical density (OD) readings obtained for differentiated cultures minus the OD reading of their undifferentiated counterparts (baseline values).

2.5 Immunolabelings and analyses on tissue cryosections

Immunolabelings were performed on tissue samples embedded in OCT compound (Tissue-Tek, Sakura Finetek, Torrance, CA, USA) and frozen at -80°C. Height µm thick acetone-fixed cross-sections were labeled with primary antibodies diluted in 1% w/v bovine serum albumin (BSA, Sigma) in phosphate buffered saline (PBS) for 45 min at RT, rinsed in PBS and then incubated for 30 min with secondary antibodies. Negative controls were performed by incubating tissue sections with a murine IgG1 isotypic antibody (Dako, Burlington, ON, Canada). Primary antibody was a mouse monoclonal antibody (IgG1) against human CD31 (Chemicon/Millipore, Temecula, CA, USA) and secondary antibody was a rabbit anti-murine IgG (H+L)-coupled Alexa 594 (Molecular Probes/Life Technologies, Burlington, ON, Canada). Hoechst 33258 (Sigma, 5 mg/ml) counterstaining was performed for 10 min in order to visualize nuclei. Pictures were acquired on an epifluorescence Nikon Eclipse E600 microscope equipped with a Sensys digital camera. Cryosections were first used to evaluate the total number of $CD31^+$ structures per field as well as the number of $CD31^+$ structures featuring a visible lumen. The internal surface area of each visible lumen was also measured and an estimated tubule diameter was calculated from it. These analyses were performed on tissues produced from different donors (N=2) for which 2-3 tissues of each condition were reconstructed. A minimum of 20 fields per sample was assessed (60 fields per condition).

2.6 Confocal imaging and analyses

For confocal imaging on whole-mount tissues, the immunolabeling protocol described below has been inspired from Dent et al., Dickie et al. and Zucker [27-29]. Thus, formalin-fixed free-floating tissue samples (about 9 mm^2) were dehydrated following incubations in 50% and 100% methanol solutions successively before being permeabilized in Dent's fixative (75% methanol, 25% DMSO) for two hours at room temperature and incubated overnight in 1:3 Dent's fixative and H_2O_2 30% solution at 4°C. Rehydration occurred with successive incubations in methanol 50% and in PBS before incubation at 4°C for 48h in 1% w/v BSA solution containing sheep anti-human CD31 (R&D Systems, Minneapolis, MN, USA, AF806, 2 µg/mL) and rabbit anti-human laminin (Abcam, AB1575, 7.3 µg/mL) primary antibodies, or isotypic sheep (Millipore) and rabbit (R&D Systems) antibodies as negative controls. After being washed in PBS to remove non-specific binding, samples were incubated with donkey anti-sheep IgG-coupled Alexa 633 (A-21100) and donkey anti-rabbit IgG-coupled Alexa 488 (A-21206) secondary antibodies (Molecular Probes) in 1% w/v BSA for 48h at 4°C. Labeled tissues were washed three times in PBS and dehydrated as previously described. Optical clearing of tissues was performed by successive incubations in 33%, 66% and 100% methylsalicylate (Sigma) solutions before being mounted in methylsalicylate and sealed with nail varnish.

Confocal microscopy allowed to acquire images of a large surface area (928.38 µm x 928.38 µm) and to observe capillary networks through the thickness of the tissues (63 ± 13 µm). Capillary network analysis was performed on a total of 17 reconstructed adipose and 18 connective tissue samples produced from 3 different cell populations with up to 3 tissues per condition. Images were acquired with a Zeiss LSM700 scanning laser confocal microscope and image software (2011, Carl Zeiss MicroImaging GmbH, Jena, Germany). Capillary network volume analyses were performed on the entire tridimensional (3D) renderings of confocal microscope images for

each tissue sample with the Imaris 7.0.0 Bitplane software. The vascular structures under 1 000 μm^3 were not considered. Frequency distribution determination was performed on selected intervals of volumes for the vascular structures on 3D reconstructed images. The same labelling process was performed on formalin-fixed human native adipose tissue samples (about 9 mm^3) to allow the comparison to human fat. Two to four samples from 4 different donors were analysed as described above for a similar surface area (928.38 x 928.38 µm) while an average of 92 ± 29 µm tissue thickness was analyzed.

Confocal images were also processed using Zen software (Zeiss) to obtain 2D representations of initial 3D images by applying a « Maximum Intensity Projection » method. Capillary mean diameters were measured on those 2D representations of confocal acquisitions with the ImageJ software. Briefly, each capillary diameter was obtained by the mean of 5 measures per capillary. Then, between 10 and 20 representative capillary diameters were measured per tissue sample for a total of 40-120 capillary diameters per population, per condition (adipose or connective tissues) from which the 40 highest diameters were used to calculate the mean capillary diameter.

2.7 Quantification of secreted products from reconstructed tissues

ELISA assays for human adipokines and bioactive molecules (leptin, angiopoietin-1 (Ang-1), plasminogen activator inhibitor-1 (PAI-1), hepatocyte growth factor (HGF), vascular endothelial growth factor (VEGF), angiopoietin-2 (Ang-2) were used as per manufacturer's instructions to establish the secretion profile of the reconstructed tissues during their production (Duosets, R&D systems). Supernatants (mean of 48h incubation) were harvested at different time-points during tissue production and stored at -80°C until assays were performed. Controls consisted of same complete media incubated in absence of cells. Analyses were performed for 2-7 different cell

populations per time point, with 1-4 sheets or tissues per condition. Some assays were repeated twice. Results are expressed as pg/μg of total protein per reconstructed sheet or tissue. The total protein content of the supernatants were determined by BCA protein assay (Pierce, Rockford, IL, USA) and used to normalize quantification of secreted products. Reagents were added as specified by manufacturer's instructions to proper supernatant dilutions and standards, then incubated for one hour at 37°C before reading at 562 nm using a SpectraMax Plus spectrometer with SoftmaxPro Ver 4.7.1.

2.8 Statistical analyses

Data are represented as mean ± SEM. Statistical comparisons were made using the GraphPad Prism 6 software (GraphPad Software Inc., LaJolla, CA, USA) and are specified in the figure legends (One-way ANOVA, One-sample *t* test) unless unpaired *t* tests were used. When mean results (same three combined cell populations) were compared, then paired *t* tests were applied. The confidence interval was set at 95% ($P<0.05$).

3. RESULTS

3.1 Defining optimal conditions for production of microvascularized tissues

First, we aimed to develop a protocol enabling reconstruction of both connective (hrCT) and adipose (hrAT) tissues containing a capillary network *in vitro* (Fig.1). After optimization, successful production of hrCT and hrAT enriched in hMVEC was achieved. Seeding of hMVEC onto the tissue sheets was performed at day 21 of culture, namely 9 days before their superposition (3 cell sheets) followed by further cultivation for 12 days (Fig. 1). While adipocyte presence is easily noticed among matrix elements on tissue histological cross-sections (Fig. 2B vs A), constructs enriched with hMVEC were very similar to their counterparts into which no hMVEC were incorporated (Fig. 2D vs B). While some tubule-like structures cross-sections (lumen) could sometimes be identified in the reconstructed tissues (Fig. 2C-D, arrowheads), their detection was highly difficult in presence of adipocytes (Fig. 2D). The latter appear as rounded void spaces resulting from lipids extracted during tissue processing. Interestingly, neither adipogenic differentiation nor hMVEC addition impacted of tissue thickness (Fig. 2E). Moreover, hMVEC seeded and cultured during 8 days on these cell sheets containing 14 day-differentiated adipocytes at the time of seeding did not impact on final lipid accumulation as determined by neutral lipids quantification after ORO staining (Fig. 2F, H). This is important, because protocols for production of prevascularized hrAT must support three biological processes in parallel: optimal ECM production, adipogenic differentiation and development of capillary-like structures by endothelial cells. Finding the right coordinated sequence for cell seeding and specialized media supplementations (adipogenic induction vs hMVEC media) during tissue production is of utmost importance (Table 1). We noted that seeding hMVEC earlier during the differentiation process, on cell sheet containing young adipocytes differentiated for only 7 days, was also

compatible with adipose tissue production and did not impact on the resulting lipid accumulation (Fig. 2G). However, seeding hMVEC on cell sheets only 3 days after adipogenic induction, resulted in complete abrogation of adipocyte development (Fig. 2G). This is likely due to the EGM2 media used to support hMVEC proliferation since control EGM2 media without hMVEC also inhibited differentiation on its own (Fig. 2G).

3.2 Revealing the endothelial networks formed in presence or absence of adipocytes

3.2.1 Analysis of endothelial structures on tissue cryosections

Immunolabelings on thin tissue cross-sections for the cell surface marker CD31 expressed by vascular cells including endothelial cells [30] revealed that hMVEC reorganized themselves to form tubular structures when surrounded by ECM (Fig. 3, arrows). Importantly, CD31 expression was not detected in tissues that were not seeded with endothelial cells (Fig. 3G). As expected from our culture conditions of expanded cells at passage 3, no spontaneous differentiation of ASCs into CD31-expressing cells or no remaining AT-derived endothelial cells were observed. While the total number of CD31-expressing structures remained the same between connective and adipose tissues (Table 2), structures featuring a defined internal space (lumen) (Fig. 3C, E arrows) were more numerous for adipose tissues. Namely, the mean percentage of such tubular structures on these labeled tissue cross-sections was twice higher in presence of adipocytes (Table 2). This analysis was performed according to classical observations of multiple sequential cryosections which is time-consuming and dependent on the sectioning angle. Therefore, the presence of the numerous CD31-expressing structures within hrCT and hrAT was best revealed using confocal microscopy after labelings of whole-mount samples (Fig. 4A, G). Staining for laminin (Fig. 4B, H) revealed the presence of a basement membrane around adipocytes (Fig. 4J,

arrow) as well as lining the external surface of capillary-like structures (Fig. 4J, arrowhead). In absence of adipocytes, the presence of laminin-covered capillary-like structures is better revealed among the CD31-expressing vascular structures (Fig. 4D, arrowheads). Additional examples of capillary-like structures formed in hrCT (Fig. 4E, F) and hrAT (Fig. 4K, L) are shown. These images were taken at specific focal positions (Z axis) of confocal images and highlight the diversity of capillary diameters and morphologies found in the reconstructed tissues, which is reminiscent of the vascular network observed within human adipose tissue samples (Fig. 4M, N).

3.2.2 Imaging and quantification of the networks using confocal microscopy

This imaging method allowed the evaluation of larger tissue surface areas ensuring a more representative assessment of the structure distribution in these tissues. The extent of the capillary-like network and its morphology could easily be visualized and then rendered as 3D images for detailed software analysis. A slight difference was noted in the global appearance of the networks created by hMVEC in presence of adipocytes, with mesh-like regions that were not present among the more « elongated » network seen within the connective tissues devoid of adipocytes (Fig. 4G vs A). Analyses using Imaris software provided more quantitative data. The total volume occupied by the network was 6.4 ± 0.9% for hrCT and 5.2 ± 0.3% for hrAT indicating no significant difference in the total volume of vessels (Fig. 5A). Moreover, this percentage was closely related to human adipose tissue samples for which 6.8 ± 1.2% of the total tissue volume consisted of vessels. The total volume occupied by endothelial structures of the reconstructed tissues was then subdivided into specific ranges of structure's volumes as illustrated on Fig. 5B. Software parameters allowed to determine individual structure volumes that could be visualized (highlighted in white) and quantified. Frequency distribution for these volume intervals was quite similar between connective and adipose tissues for all the intervals (Fig. 5C).

3.2.3 Determination of capillary's mean diameter

Finally, ImageJ analyses of confocal images were used to estimate the average diameter of capillary-like structures in presence or absence of adipocytes (Fig. 6A). Mean diameters varied depending on the cell population initially used to produce connective and adipose tissues (Fig. 6B). However, after paired analysis of the data combined from three distinct cell populations, a 1.2x fold non-significant tendency was observed (Fig. 6B, Mean). This is also in accordance with the results obtained after the more traditional cryosection analysis for which the average diameter was estimated from measurements of the internal lumen cross-sections and tended to be 28% superior in presence of adipocytes (Table 2).

3.3 Influence of the tissue microenvironment: kinetics of bioactive molecule secretion

The presence of basement membrane components such as laminin (Fig. 4B, H) and collagen type IV (not shown), likely provided essential cues favoring the endothelial network development. In addition, soluble factors secreted by ASCs and/or adipocytes such as leptin, VEGF, Ang-1, HGF, and PAI-1 represent known modulators of angiogenic processes [8]. Their quantification in conditioned media (CM) would likely reflect the local environment seen by hMVEC during tissue production. Therefore we performed a detailed investigation of the secretory profiles of these molecules for hrCT and hrAT at major steps of tissue reconstruction *in vitro* (Fig. 7).

3.3.1 Impact of endothelial cells within the substitutes

First, the presence of hMVEC *per se* did not impact the secretory profiles of leptin, Ang-1, HGF and PAI-1 from hrCT (Fig. 7A, B, D, E) or hrAT (Fig. 7F, G, I, J), with none to slight

modulation of VEGF secretion depending on the time-point (Fig. 7C, H). This was evaluated by comparing tissues enriched in hMVEC with their reference tissues devoid of hMVEC but cultured in the same coculture EGM2-containing media at day 30 and 42 of culture (Fig. 7). At day 21 (before hMVEC seeding) and 30 of culture, media is conditioned by cell sheets while at day 42, it is conditioned by thicker tissues reconstructed by superposition of 3 cell sheets. Importantly, endothelial cell contribution to tissue functionality was shown by detection of Ang-2 secretion. Ang-2 was detected only in hMVEC-enriched conditioned media at levels ranging from 1.16 ± 0.08 to 0.31 ± 0.02 pg/µg protein for reconstructed connective and adipose tissues respectively (at day 42, n=3).

3.3.2 Impact of adipocytes

The presence of adipocytes likely impacted on tissue microenvironment through their various secretory products (Fig. 7, hrAT vs hrCT). Conditioned media harvested immediately before hMVEC seeding (d21) is indicative of the local environment seen by these cells on the two types of tissue. Namely, hMVEC seeded onto adipose sheets in comparison to connective sheets (ratio hrAT/hrCT, Fig. 8A day 21) were generally in presence of elevated amounts of leptin (15x), Ang-1 (3.4x non-sig), VEGF (2.0x, non-sig) and HGF (1.7x) while PAI-1 was secreted at similar levels by connective and adipose tissues at this time-point.

3.3.3. Impact of coculture media

However, this profile drastically changed upon co-culturing with hMVEC (Fig. 8A, day 30 and 42) showing a general decrease of the hrAT/hrCT ratio over time for all molecules except PAI-1. Surprisingly, culture using the endothelial EGM2-media alone, even in absence of hMVEC, resulted in similar decreased detection of leptin in hrAT as well as decreased Ang-1 detection for

hrCT and hrAT, at both time-points investigated (Fig. 8B, C and Figure 7B, F, G). Combined with increased levels of VEGF, HGF and PAI-1 in these same conditioned media (Fig. 8B, C and Fig. 7C-E, H-J), the resulting microenvironment become rather similar with time, attenuating the initial differences for these molecules between adipose and connective tissues during capillary-like network formation.

4. DISCUSSION

Various strategies have been designed over the years to ensure adequate vascularization of voluminous tissues upon grafting [31, 32]. Conditions promoting both angiogenesis and adipogenesis *in vivo* are being investigated including growth factor stimulation, the use of inductive biomaterials and combinations of diverse modalities [33-39]. The concept of producing *in vitro* tissues featuring a preformed capillary network in order to favor inosculation once grafted is also developed for a variety of tissue types and engineering models [19, 40-42]. In particular, microvascularized tissues including skin and bladder have been produced from dermal fibroblasts and endothelial cells [human umbilical vein endothelial cell (HUVEC) and microvascular] [20, 43, 44] using a cell sheet technology adapted here to produce adipose substitutes from ASCs. Adipocytes, stromal and endothelial cells are major components of native adipose tissue. In this study, hASC and hMVEC were extracted, amplified separately in culture and later combined to produce an *in vitro* engineered adipose tissue featuring a preformed capillary network. Specific challenges are associated with hrAT production such as concomitant matrix production, lipid accumulation and endothelial cell tubule formation. Finding the right coordinated sequence for cell seeding and specialized media supplementations (adipogenic induction vs hMVEC media) during tissue production is of utmost importance. While some model systems first culture HUVECs on the scaffolds and then add mesenchymal cells that have been predifferentiated or not [45], here we added hMVEC onto cell sheets already rich in matrix components and/or adipocytes and then produced cohesive thicker tissues through sheet superposition. We noted that the sequence of adipogenic induction and hMVEC seeding that was conducive both to adipocyte maturation and tubule formation was obtained when performed at least 3 days apart, respectively.

Some advantages of this tissue-engineered model include that scaffolding elements are of human origin and therefore ECM components reflect the natural composition of native adipose tissue. Indeed, ASCs stimulated with ascorbic acid and serum produce a complex ECM including fibronectin and collagens type I and V while basement membrane components including laminin accumulate upon adipogenic induction [23, 24]. Collagen type IV has also been shown to be highly expressed around adipocytes in adipose sheets [46]. The rather efficient formation of capillary-like networks by hMVEC within our reconstructed tissues is likely mediated by the combination of signals from the ECM, the cells themselves and their soluble secreted products.

The extent of the networks formed *in vitro* was best visualized by confocal microscopy on whole-mount specimens which allowed the examination of rather large tissue areas as well as quantitative characterization of the endothelial structures. Such three-dimensional imaging provides pertinent informations concerning morphology and the overall distribution of the networks within the tissues, which cannot be easily achieved following classical serial labeling of cryosections. Such analysis of hrCT and hrAT tissue samples determined that their total volume occupied by CD31-expressing structures were similar to the value obtained for native AT samples. Moreover, during the span of 21 days covered from hMVEC seeding to tissue analysis, endothelial cells attached, proliferated, migrated and assembled themselves into nascent tubular structures surrounded by laminin and secreting Ang-2, both for hrCT and hrAT. Ang-2 is stored in endothelial cell Weibel-Palade bodies and such expression suggests it could act in an autocrine manner to regulate endothelial cell states of quiescence and responsiveness to stimuli through TIE2 receptor [47].

Another strength of the experimental design relies on the fact that the same ASCs populations were used, under similar culture conditions, to produce paired tissues induced or not towards adipogenesis. Numerous investigations highlight the major contributions of secreted molecules from ASCs as well as adipocytes to their microenvironment [48, 49]. In particular, it is now well accepted that adipocytes are dynamic contributors to metabolic regulation via active production of adipokines, cytokines and growth factors [50]. Therefore, we wanted to ascertain if metabolically-active adipocytes would have an impact on the resulting capillary-like network *in vitro.* Considering the different soluble microenvironment as well as the distinct topology of rounded lipid-filled adipocytes that is seen by the seeded hMVEC during network formation, more significant morphological differences between hrCT and hrAT networks could have been expected. However, a study that evaluated the early events occurring after endothelial cell seeding onto adipose sheets showed that if HUVEC first attached to adipocytes, they then migrated rapidly (between 2h to 5h) to the surrounding stromal cells before developing into tube-like structures over time [46]. It is therefore possible that in our engineered tissues, the remaining ASCs that did not differentiate into adipocytes upon induction actively contributed to the network formation as vascular support cells.

The functionality of the cells within the reconstructed tissues during the culture period is demonstrated by the sustained production of adipokines and growth factors *in vitro*. At the time of hMVEC seeding (day 21 of culture), there were indeed differential expression levels of leptin, Ang-1 and HGF between hrCT and hrAT. Brieftly, leptin was strongly detected in media conditioned by hrAT. This adipocyte-derived molecule has been reported to stimulate migration and proliferation of endothelial cells *in vitro*, as well as angiogenesis *in vivo* [51]. Ang-1 mediates its actions through binding to the endothelial cell TIE2 receptor. It has been reported to

be chemotactic for endothelial cells [52] and involved in processes leading to vessel stabilization and maturation [53]. HGF, via c-Met receptor binding, is an important angiogenic factor for vessels growth and remodeling that stimulates proliferation and migration of endothelial cells [54]. The important effects of the endothelial EGM2 containing coculture media on hrCT and hrAT secretomes contributed to mask the potential adipocyte-related differences in the surrounding microenvironment. The important decrease in leptin secretion we observed in hrAT is in accordance with the recently reported decrease in leptin gene expression in another adipose engineering system using EGM2-containing coculture media [55]. Of course, one of the most studied and potent angiogenic factor is VEGF. The increase in VEGF and HGF we noted in presence of coculture media (Fig. 8) could likely be attributed to epidermal growth factor (EGF) presence in this endothelial media, since EGF has been previously shown to increase VEGF, HGF and stromal cell-derived factor-1 (SDF-1) secretion by ASCs [56]. Such an increase in VEGF expression mediated by EGM2 media could actually be beneficial overall, favoring the development CD31+ structures as well as increased platelet-derived growth factor (PDGF) levels in conditioned media [57].

While these growth factors and adipokines all have the properties to modulate angiogenic processes, they only represent selected examples from the tissue secretomes and their potential synergistic/antagonistic effects should not be underestimated. Also it cannot be excluded that adipocyte presence might have had an effect during the earlier phases of tissue reconstruction. But importantly, despite these changes in the secreted microenvironment related to the choice of coculture media, premicrovascularized hrAT featuring substantial adipocytes were produced, thereby recreating the adipose tissue context.

5. CONCLUSION

In summary, this work indicates that both connective and adipose human substitutes produced by the self-assembly method of tissue engineering can sustain the development of robust and stable capillary networks *in vitro*. These networks were quite similar in presence or absence of adipocytes under the specific culture conditions used for tissue production. Combined with a detailed characterization using confocal imaging, these substitutes represent excellent models for studying molecules that are putative angiogenic and/or adipogenic modulators. The functionality and ease of manipulation of these reconstructed tissues also contribute to their promising use as substitutes for soft-tissue regeneration.

Acknowledgements

We thank V. Trottier, M. Vermette, J. Desjardins, S. Pouliot and V. Racine for technical assistance during tissue production and analysis. We are grateful to V. Moulin and S. Chabaud for providing skin microvascular endothelial cells. This work was supported by the Canadian Institutes of Health Research (CIHR) grants #84368 and #111233. We acknowledge the support of the Centre de recherche du CHU de Québec du Fonds de recherche du Québec–Santé (FRQS) and of the Réseau ThéCell du FRQS. The confocal imaging system was obtained through the Fonds des leaders program from Canada Foundation for Innovation (CFI) to J. Fradette. K. Aubin received a studentship from Fonds de recherche du Québec - Nature et technologies (FQRNT). M. Proulx received studentships from National Science and Engineering Research Council (NSERC), FRQS and the Canadian Federation of University Women (CFUW). J. Fradette is a FRQS career award scholar.

Disclosures

No competing financial interests exist for the authors.

Table 1. Media composition at different steps of tissue production

Time in culture (day)	Culture step	Connective (hrCT)	Adipose (hrAT)
0-7	Expanding cells in 6-well plates	DH medium (1:1 DMEM : Ham's F12) + 10% FCS + 250 µM AsA	DH medium (1:1 DMEM : Ham's F12) + 10% FCS + 250 µM AsA
7	Induction of adipogenesis	DH medium (3% FCS) + 0.038% DMSO + 250 µM AsA	DH medium (3% FCS) + 100 nM insulin, 0.2 nM T3, 1 µM dexamethasone, 0.25 mM IBMX and 1 µM rosiglitazone + 250 µM AsA
21-42 (-hMVEC, -EGM2)	Culture without hMVEC	DH medium (10% FCS) + 250 µM AsA	Adipogenic maintenance medium [DH medium (10% FCS) + 100 nM insulin, 0.2 nM T3, 1 µM dexamethasone] + 250 µM AsA
21-42 (+ hMVEC, +EGM2)	Coculture with hMVEC	1:1 DH (10% FCS) : EGM2 (5% FBS) + 250 µM AsA	1:1 Adipogenic maintenance medium : EGM2 (5% FBS) + 250 µM AsA
21-42 (-hMVEC, +EGM2)	Culture without hMVEC (control)	1:1 DH (10% FCS) : EGM2 (5% FBS) + 250 µM AsA	1:1 Adipogenic maintenance medium : EGM2 (5% FBS) + 250 µM AsA

Table 2. Comparison of CD31-labeled structures detected on hrCT and hrAT tissue cryosections

Tissue type	Total number of $CD31^+$ structures	Number of tubular $CD31^+$ structures	Mean % of tubular structures	Measured internal lumen (μm^2)	Estimated mean diameter (μm)
hrCT	7.9 (2.7)	1.7 (0.8)	17.9 (4.2)	180.7 (13.0)	14.0 (0.5)
hrAT	7.5 (2.3)	2.6 (0.7)	35.2 (4.6)*	304.1 (59.0)	17.9 (2.3)
			p= 0.0381	p= 0.2000	p= 0.2508

Data is expressed as mean per field (SEM)

* $p < 0.05$

FIGURE LEGENDS

Figure 1: **Schematic representation of tissue production according to the self-assembly method of tissue engineering**. Both connective (hrCT) and adipose (hrAT) reconstructed tissues were produced using the self-assembly approach of tissue engineering based on enhanced matrix deposition leading to cell sheet formation upon cell stimulation with ascorbic acid and serum. Incorporation of endothelial cells in the constructs was achieved by seeding the upper surface of individual cell sheets that were then superimposed to create thicker tissues. Accordingly, four types of tissues were generated since connective and adipose tissues without hMVEC were also produced following the same steps but replacing cells with respective media only.

Figure 2: Reconstructed tissue characterization. (A-D) Representative histological appearance of engineered constructs. Tissue cross-sections were stained with Masson's trichrome for human reconstructed A) connective and B) adipose tissues, and their respective counterparts seeded with endothelial cells in C and D, respectively. Higher magnifications of boxed areas are shown on the bottom right with arrowheads pointing to putative lumen structures. E) Adipogenic differentiation or hMVEC incorporation did not affect tissue thickness. F) Co-culturing endothelial cells for 8 days on reconstructed adipose sheets containing adipocytes differentiated for 14 days did not interfere with adipocyte maturation. G) hMVEC seeded onto cell sheets containing younger adipocytes (d7 of differentiation) did not affect lipid accumulation (over 14 days of culture) while it abrogated adipocyte development when seeded only 3 days after adipogenic induction. H) Typical appearance after Oil Red O staining of an adipose cell sheet after 22 days of *in vitro* differentiation. Bars: 50 μm; C, D boxed areas: 10 μm.

Figure 3: Detection of tubular structures formed by hMVEC within reconstructed tissues. Transversal cryosections of A-B) connective and C-F) adipose reconstructed tissues seeded with hMVEC after immunolabeling for CD31. Lumen-like structures (arrows) can be identified more easily on adipose tissue sections. G-H) Adipose tissues not enriched in hMVEC do not reveal CD31-expressing cells or structures. B, D, F, H are corresponding phase contrast images of A, C, E, G, respectively. Bar: 100 µm.

Figure 4: Confocal imaging of capillary-like networks within engineered tissues. Reconstructed (A-F) connective and (G-L) adipose tissue whole-mount samples were immunolabeled for (A, G) CD31 and (B, H) laminin and stacked images acquired by confocal microscopy are shown (top view). (C, I) represent merging of the labelings. (D, J) Higher magnification images indicating laminin presence around capillaries (D, J, arrowheads) and adipocytes (J, arrow). Details of capillary-like tubules present within reconstructed (E, F) connective and (K, L) adipose tissues illustrate the diversity in size of CD31-expressing structures, also observed for samples of native human adipose tissue (M, N). Bars: A-C, G-I: 150 µm; D-F, J-N: 50 µm.

Figure 5: Characterization of the endothelial networks. A) Quantification of the tissue volume occupied by CD31-expressing structures for tissues reconstructed using ASCs from three different donors. B) 3D renderings of confocal images used for software analysis. Representation of structures present within the specified volume intervals are shown in white. C) Frequency distribution of the structures according to the specified intervals for hrCT and hrAT (mean of three donors). Unpaired *t* tests, * : $p < 0.05$. Bar: 100 µm

Figure 6: Determination of capillary diameter. A) Representation of measurements performed on 2D renderings of confocal images. B) Mean capillary diameter of CD31-labeled hrCT and hrAT reconstructed using ASCs from three different donors. * : $p < 0.05$, **** : $p < 0.0001$. Bars: A) 100 µm; A') 50 µm.

Figure 7: Kinetics of adipokine secretion during production of the reconstructed tissues. Adipokine detection in 48h-conditioned media of (A-E) connective and (F-J) adipose tissues enriched or not with hMVEC and in presence or not of EGM2-containing coculture media. Quantification was performed at important steps of sheet/tissue production namely at day 21 of culture just before endothelial cell seeding, at day 30 before cell sheet superposition into thicker tissues as well as at day 42 before the reconstructed tissues were harvested for analysis. Unpaired *t* tests were performed to evaluate the effect of each parameter on protein secretion: the presence of hMVEC in the model and the addition of EGM2 medium in coculture. **** : $p < 0.0001$, *** : $p < 0.001$, ** : $p < 0.01$, * : $p < 0.05$, N = 2-7 different ASC donors with up to 4 tissues per condition (connective or adipose tissues).

Figure 8: **Impact of EGM2-containing media on secretory profiles**. A) Differential expression of leptin, Ang-1, VEGF, HGF and PAI-1 between reconstructed adipose and connective tissues at important steps of tissue production (ratio hrAT/hrCT, mean ± SEM for tissues from 1-4 different ASC donors). Before hMVEC seeding (d21), adipose sheets secreted higher amounts of leptin, Ang-1 and HGF. This was attenuated during the following culture time in EGM2-containing coculture media. B-C) The impact of EGM2-media alone was further evaluated during a side by side comparison comparing the secretory profiles of tissues reconstructed using basic growth/adipocyte maintenance media or endothelial EGM2-containing coculture media. EGM2

coculture media induced important variations at B) day 30 of culture (9 days of EGM2 presence, cell sheets) as well as C) day 42 of culture (21 days of EGM2 presence, reconstructed tissues) (N=1 cell population, repeated twice with up to 4 tissues per condition). # indicates significance from ratio of 1 (One-sample *t* test). For Ang-1, VEGF, HGF et PAI-1: * : $p < 0.05$, one-way ANOVA followed by Tukey's post-test. For leptin: unpaired *t* test was performed between d30 and d42 since N=1 donor (in triplicate) at d21. *** : $p = 0.0007$.

REFERENCES

[1] Rupnick MA, Panigrahy D, Zhang CY, Dallabrida SM, Lowell BB, Langer R, et al. Adipose tissue mass can be regulated through the vasculature. Proc Natl Acad Sci U S A 2002;99:10730-10735.

[2] Miranville A, Heeschen C, Sengenes C, Curat CA, Busse R, Bouloumie A. Improvement of postnatal neovascularization by human adipose tissue-derived stem cells. Circulation 2004;110:349-355.

[3] Bouloumié A, Galitzky J. Angiogenesis in Adipose Tissue. In: Bastard J-P, Fève B, editors. Physiology and Physiopathology of Adipose Tissue: Springer Paris; 2013. p. 27-38.

[4] Crandall DL, Hausman GJ, Kral JG. A review of the microcirculation of adipose tissue: anatomic, metabolic, and angiogenic perspectives. Microcirculation 1997;4:211-232.

[5] Nishimura S, Manabe I, Nagasaki M, Hosoya Y, Yamashita H, Fujita H, et al. Adipogenesis in obesity requires close interplay between differentiating adipocytes, stromal cells, and blood vessels. Diabetes 2007;56:1517-1526.

[6] Rehman J, Traktuev D, Li J, Merfeld-Clauss S, Temm-Grove CJ, Bovenkerk JE, et al. Secretion of angiogenic and antiapoptotic factors by human adipose stromal cells. Circulation 2004;109:1292-1298.

[7] Trayhurn P. Endocrine and signalling role of adipose tissue: new perspectives on fat. Acta Physiol Scand 2005;184:285-293.

[8] Cao Y. Angiogenesis modulates adipogenesis and obesity. J Clin Invest 2007;117:2362-2368.

[9] Harwood HJ, Jr. The adipocyte as an endocrine organ in the regulation of metabolic homeostasis. Neuropharmacology 2012;63:57-75.

[10] Fain JN, Madan AK, Hiler ML, Cheema P, Bahouth SW. Comparison of the release of adipokines by adipose tissue, adipose tissue matrix, and adipocytes from visceral and subcutaneous abdominal adipose tissues of obese humans. Endocrinology 2004;145:2273-2282.

[11] Zuk PA, Zhu M, Mizuno H, Huang J, Futrell JW, Katz AJ, et al. Multilineage cells from human adipose tissue: implications for cell-based therapies. Tissue Eng 2001;7:211-228.

[12] Murphy MB, Moncivais K, Caplan AI. Mesenchymal stem cells: environmentally responsive therapeutics for regenerative medicine. Exp Mol Med 2013;45:e54.

[13] Nguyen A, Pasyk KA, Bouvier TN, Hassett CA, Argenta LC. Comparative study of survival of autologous adipose tissue taken and transplanted by different techniques. Plast Reconstr Surg 1990;85:378-386; discussion 387-379.

[14] Konczalik W, Siemionow M. Experimental and clinical methods used for fat volume maintenance after autologous fat grafting. Ann Plast Surg 2014;72:475-483.

[15] Tanzi MC, Fare S. Adipose tissue engineering: state of the art, recent advances and innovative approaches. Expert Rev Med Devices 2009;6:533-551.

[16] Choi JH, Gimble JM, Lee K, Marra KG, Rubin JP, Yoo JJ, et al. Adipose tissue engineering for soft tissue regeneration. Tissue Eng Part B Rev 2010;16:413-426.

[17] Bauer-Kreisel P, Goepferich A, Blunk T. Cell-delivery therapeutics for adipose tissue regeneration. Adv Drug Deliv Rev 2010;62:798-813.

[18] Laschke MW, Harder Y, Amon M, Martin I, Farhadi J, Ring A, et al. Angiogenesis in tissue engineering: breathing life into constructed tissue substitutes. Tissue Eng 2006;12:2093-2104.

[19] Black AF, Berthod F, L'Heureux N, Germain L, Auger FA. In vitro reconstruction of a human capillary-like network in a tissue-engineered skin equivalent. FASEB J 1998;12:1331-1340.

[20] Rochon MH, Fradette J, Fortin V, Tomasetig F, Roberge CJ, Baker K, et al. Normal human epithelial cells regulate the size and morphology of tissue-engineered capillaries. Tissue Eng Part A 2010;16:1457-1468.

[21] Vermette M, Trottier V, Menard V, Saint-Pierre L, Roy A, Fradette J. Production of a new tissue-engineered adipose substitute from human adipose-derived stromal cells. Biomaterials 2007;28:2850-2860.

[22] Fortier GM, Gauvin R, Proulx M, Vallee M, Fradette J. Dynamic culture induces a cell type-dependent response impacting on the thickness of engineered connective tissues. J Tissue Eng Regen Med 2013;7:292-301.

[23] Trottier V, Marceau-Fortier G, Germain L, Vincent C, Fradette J. IFATS collection: Using human adipose-derived stem/stromal cells for the production of new skin substitutes. Stem Cells 2008;26:2713-2723.

[24] Vallee M, Cote JF, Fradette J. Adipose-tissue engineering: taking advantage of the properties of human adipose-derived stem/stromal cells. Pathol Biol (Paris) 2009;57:309-317.

[25] Germain L, Rouabhia M, Guignard R, Carrier L, Bouvard V, Auger FA. Improvement of human keratinocyte isolation and culture using thermolysin. Burns 1993;19:99-104.

[26] Labbé B, Marceau Fortier G, Fradette J. Cell Sheet Technology for Tissue Engineering: The Self-Assembly Approach Using Adipose-Derived Stromal Cells. Adipose-Derived Stem Cells: Methods and Protocols. New York: Humana Press; 2011. p. 429-441.

[27] Dent JA, Polson AG, Klymkowsky MW. A whole-mount immunocytochemical analysis of the expression of the intermediate filament protein vimentin in Xenopus. Development 1989;105:61-74.

[28] Dickie R, Bachoo RM, Rupnick MA, Dallabrida SM, Deloid GM, Lai J, et al. Three-dimensional visualization of microvessel architecture of whole-mount tissue by confocal microscopy. Microvasc Res 2006;72:20-26.

[29] Zucker RM. Whole insect and mammalian embryo imaging with confocal microscopy: morphology and apoptosis. Cytometry A 2006;69:1143-1152.

[30] Ilan N, Madri JA. PECAM-1: old friend, new partners. Curr Opin Cell Biol 2003;15:515-524.

[31] Kannan RY, Salacinski HJ, Sales K, Butler P, Seifalian AM. The roles of tissue engineering and vascularisation in the development of micro-vascular networks: a review. Biomaterials 2005;26:1857-1875.

[32] Baiguera S, Ribatti D. Endothelialization approaches for viable engineered tissues. Angiogenesis 2013;16:1-14.

[33] Stillaert F, Findlay M, Palmer J, Idrizi R, Cheang S, Messina A, et al. Host rather than graft origin of Matrigel-induced adipose tissue in the murine tissue-engineering chamber. Tissue Eng 2007;13:2291-2300.

[34] Laschke MW, Kleer S, Scheuer C, Schuler S, Garcia P, Eglin D, et al. Vascularisation of porous scaffolds is improved by incorporation of adipose tissue-derived microvascular fragments. Eur Cell Mater 2012;24:266-277.

[35] Butler MJ, Sefton MV. Cotransplantation of adipose-derived mesenchymal stromal cells and endothelial cells in a modular construct drives vascularization in SCID/bg mice. Tissue Eng Part A 2012;18:1628-1641.

[36] Yao R, Zhang R, Lin F, Luan J. Biomimetic injectable HUVEC-adipocytes/collagen/alginate microsphere co-cultures for adipose tissue engineering. Biotechnol Bioeng 2013;110:1430-1443.

[37] Lu Q, Li M, Zou Y, Cao T. Delivery of basic fibroblast growth factors from heparinized decellularized adipose tissue stimulates potent de novo adipogenesis. J Control Release 2014;174:43-50.

[38] Traktuev DO, Prater DN, Merfeld-Clauss S, Sanjeevaiah AR, Saadatzadeh MR, Murphy M, et al. Robust functional vascular network formation in vivo by cooperation of adipose progenitor and endothelial cells. Circ Res 2009;104:1410-1420.

[39] Turner AE, Yu C, Bianco J, Watkins JF, Flynn LE. The performance of decellularized adipose tissue microcarriers as an inductive substrate for human adipose-derived stem cells. Biomaterials 2012;33:4490-4499.

[40] Magnan M, Berthod F, Champigny MF, Soucy F, Bolduc S. In vitro reconstruction of a tissue-engineered endothelialized bladder from a single porcine biopsy. J Pediatr Urol 2006;2:261-270.

[41] Correia C, Grayson WL, Park M, Hutton D, Zhou B, Guo XE, et al. In vitro model of vascularized bone: synergizing vascular development and osteogenesis. PLoS One 2011;6:e28352.

[42] Verseijden F, Posthumus-van Sluijs SJ, Farrell E, van Neck JW, Hovius SE, Hofer SO, et al. Prevascular structures promote vascularization in engineered human adipose tissue constructs upon implantation. Cell Transplant 2010;19:1007-1020.

[43] Gibot L, Galbraith T, Huot J, Auger FA. A preexisting microvascular network benefits in vivo revascularization of a microvascularized tissue-engineered skin substitute. Tissue Eng Part A 2010;16:3199-3206.

[44] Bouhout S, Perron E, Gauvin R, Bernard G, Ouellet G, Cattan V, et al. In vitro reconstruction of an autologous, watertight, and resistant vesical equivalent. Tissue Eng Part A 2010;16:1539-1548.

[45] Kang JH, Gimble JM, Kaplan DL. In vitro 3D model for human vascularized adipose tissue. Tissue Eng Part A 2009;15:2227-2236.

[46] Sorrell JM, Baber MA, Traktuev DO, March KL, Caplan AI. The creation of an in vitro adipose tissue that contains a vascular-adipocyte complex. Biomaterials 2011;32:9667-9676.

[47] Fiedler U, Scharpfenecker M, Koidl S, Hegen A, Grunow V, Schmidt JM, et al. The Tie-2 ligand angiopoietin-2 is stored in and rapidly released upon stimulation from endothelial cell Weibel-Palade bodies. Blood 2004;103:4150-4156.

[48] Kapur SK, Katz AJ. Review of the adipose derived stem cell secretome. Biochimie 2013;95:2222-2228.

[49] Salgado AJ, Reis RL, Sousa NJ, Gimble JM. Adipose tissue derived stem cells secretome: soluble factors and their roles in regenerative medicine. Curr Stem Cell Res Ther 2010;5:103-110.

[50] Fonseca-Alaniz MH, Takada J, Alonso-Vale MI, Lima FB. Adipose tissue as an endocrine organ: from theory to practice. J Pediatr (Rio J) 2007;83:S192-203.

[51] Bouloumie A, Drexler HC, Lafontan M, Busse R. Leptin, the product of Ob gene, promotes angiogenesis. Circ Res 1998;83:1059-1066.

[52] Witzenbichler B, Maisonpierre PC, Jones P, Yancopoulos GD, Isner JM. Chemotactic properties of angiopoietin-1 and -2, ligands for the endothelial-specific receptor tyrosine kinase Tie2. J Biol Chem 1998;273:18514-18521.

[53] Thurston G, Rudge JS, Ioffe E, Zhou H, Ross L, Croll SD, et al. Angiopoietin-1 protects the adult vasculature against plasma leakage. Nat Med 2000;6:460-463.

[54] Saiki A, Watanabe F, Murano T, Miyashita Y, Shirai K. Hepatocyte growth factor secreted by cultured adipocytes promotes tube formation of vascular endothelial cells in vitro. Int J Obes (Lond) 2006;30:1676-1684.

[55] Yao R, Du Y, Zhang R, Lin F, Luan J. A biomimetic physiological model for human adipose tissue by adipocytes and endothelial cell cocultures with spatially controlled distribution. Biomed Mater 2013;8:045005.

[56] Li Q, Li PH, Hou DJ, Zhang AJ, Tao CB, Li XY, et al. EGF Enhances ADSCs Secretion via ERK and JNK Pathways. Cell Biochem Biophys 2013.

[57] Kolbe M, Xiang Z, Dohle E, Tonak M, Kirkpatrick CJ, Fuchs S. Paracrine effects influenced by cell culture medium and consequences on microvessel-like structures in cocultures of mesenchymal stem cells and outgrowth endothelial cells. Tissue Eng Part A 2011;17:2199-2212.

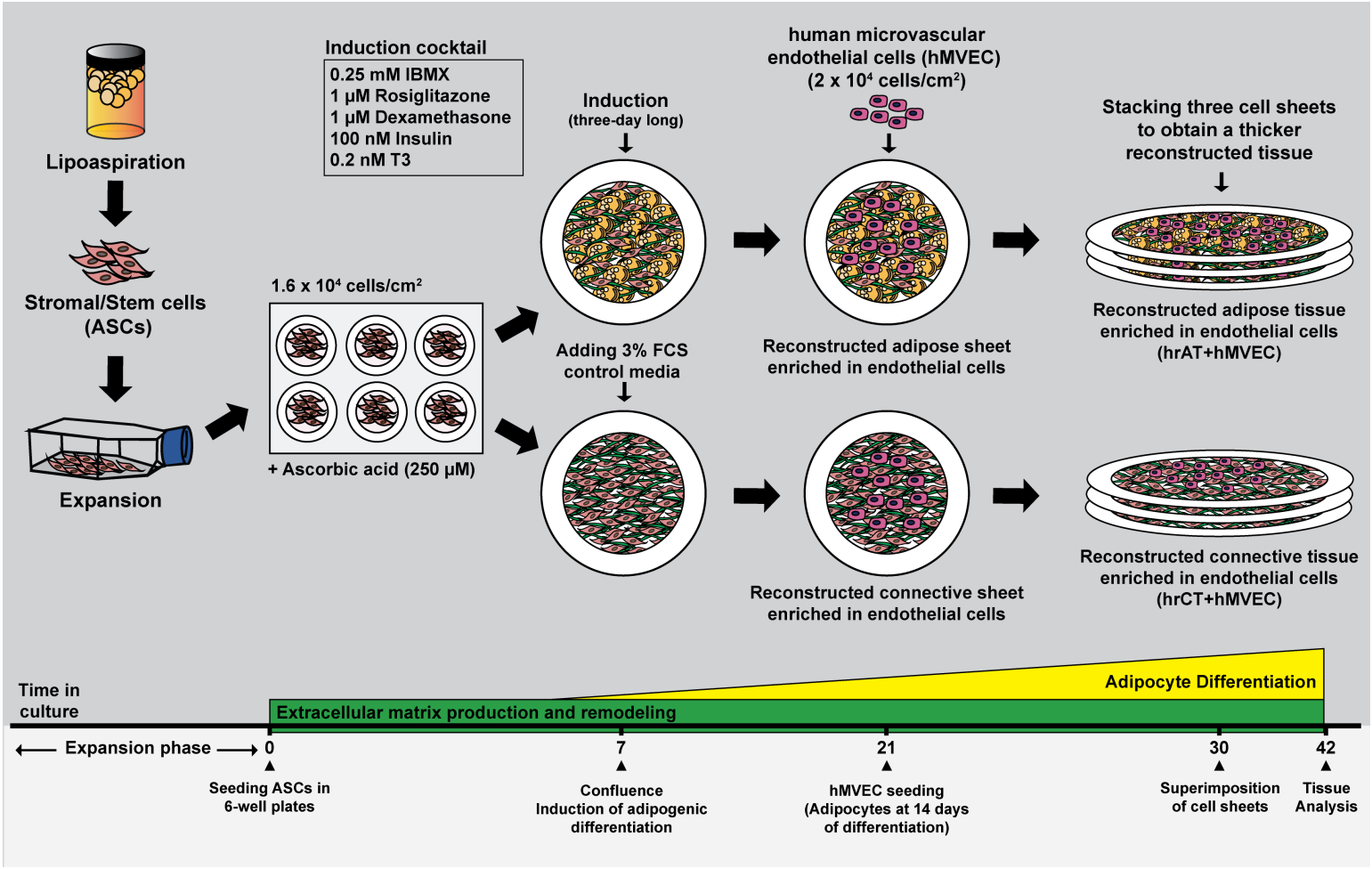
Lipoaspiration
Stromal/Stem cells (ASCs)
Expansion
Induction cocktail
0.25 mM IBMX
1 µM Rosiglitazone
1 µM Dexamethasone
100 nM Insulin
0.2 nM T3
1.6 x 10⁴ cells/cm²
+ Ascorbic acid (250 µM)
Induction
(three-day long)
Adding 3% FCS
control media
human microvascular
endothelial cells (hMVEC)
(2 x 10⁴ cells/cm²)
Reconstructed adipose sheet
enriched in endothelial cells
Reconstructed connective sheet
enriched in endothelial cells
Stacking three cell sheets
to obtain a thicker
reconstructed tissue
Reconstructed adipose tissue
enriched in endothelial cells
(hrAT+hMVEC)
Reconstructed connective tissue
enriched in endothelial cells
(hrCT+hMVEC)
Time in culture
Adipocyte Differentiation
Extracellular matrix production and remodeling
Expansion phase
0
7
21
30
42
Seeding ASCs in 6-well plates
Confluence
Induction of adipogenic differentiation
hMVEC seeding
(Adipocytes at 14 days of differentiation)
Superimposition of cell sheets
Tissue Analysis

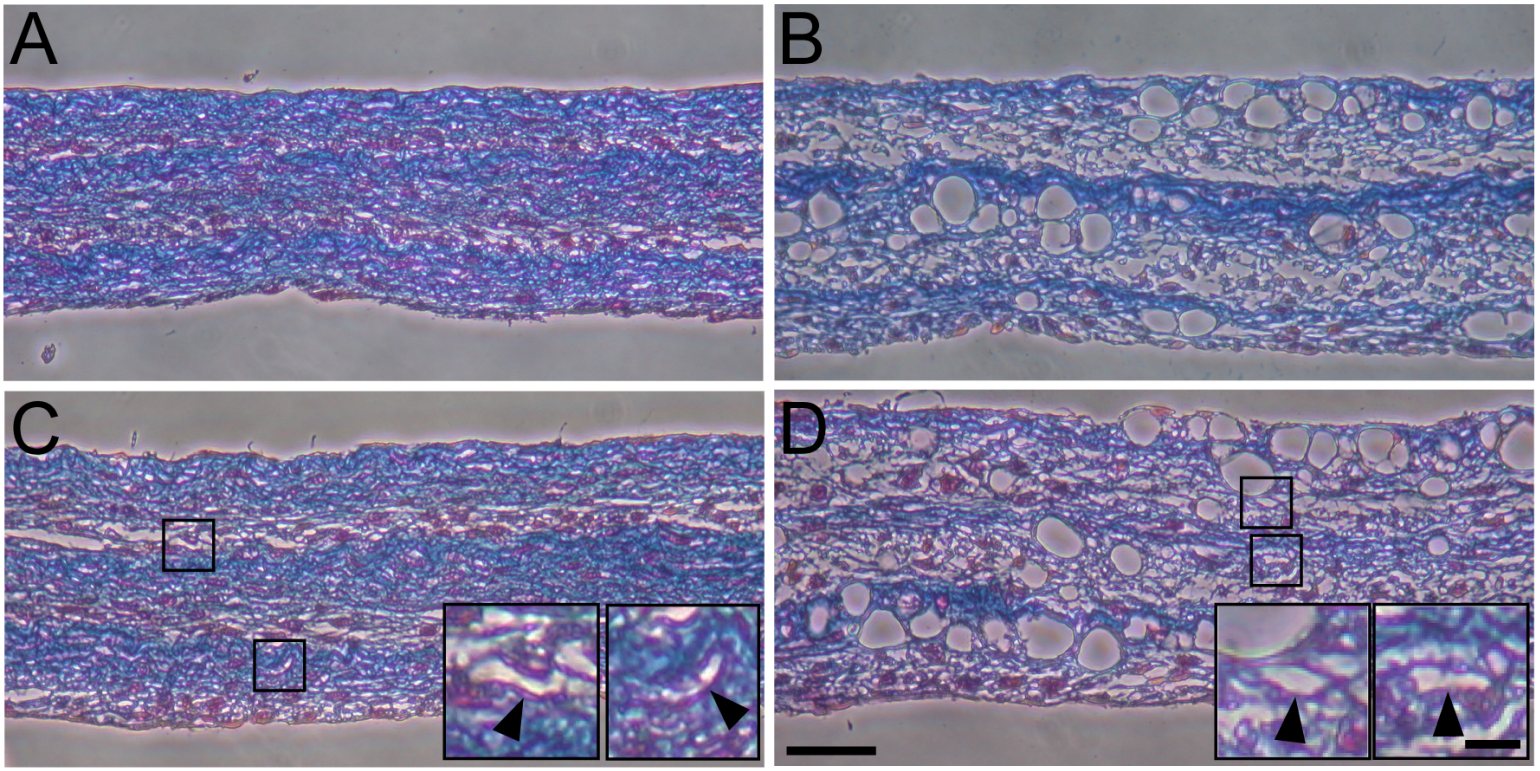
A
B
C
D

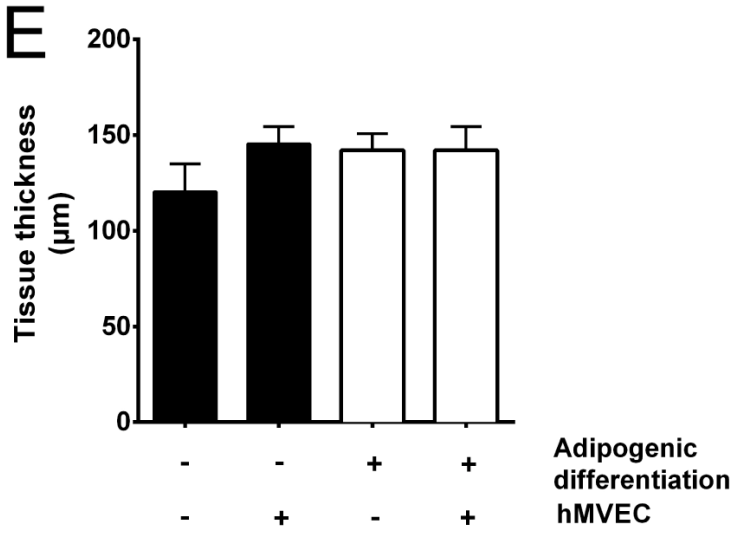
E
Tissue thickness (µm)
200
150
100
50
0
- - + +
- + - +
Adipogenic differentiation
hMVEC

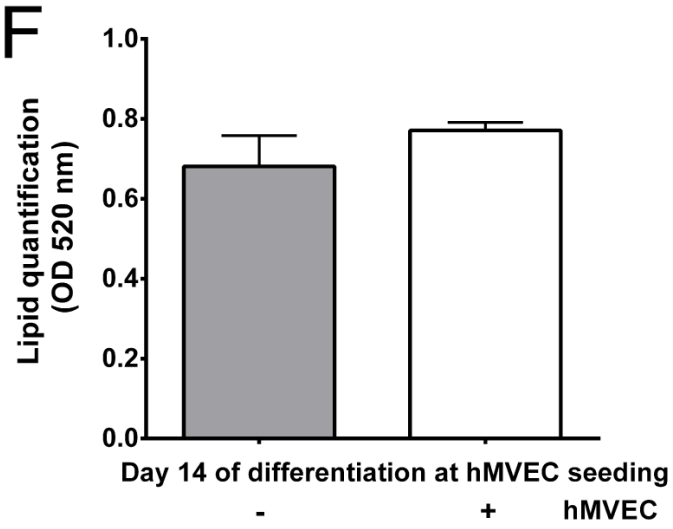
F
Lipid quantification (OD 520 nm)
1.0
0.8
0.6
0.4
0.2
0.0
Day 14 of differentiation at hMVEC seeding
- +
hMVEC

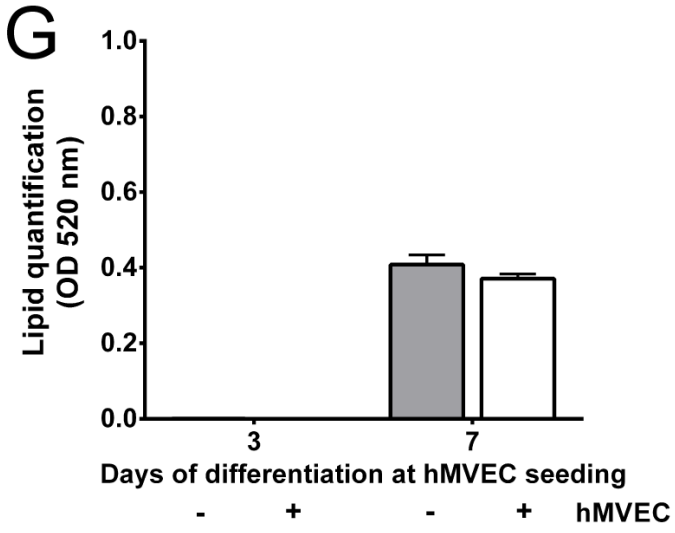
G
Lipid quantification (OD 520 nm)
1.0
0.8
0.6
0.4
0.2
0.0
3
7
Days of differentiation at hMVEC seeding
- + - +
hMVEC

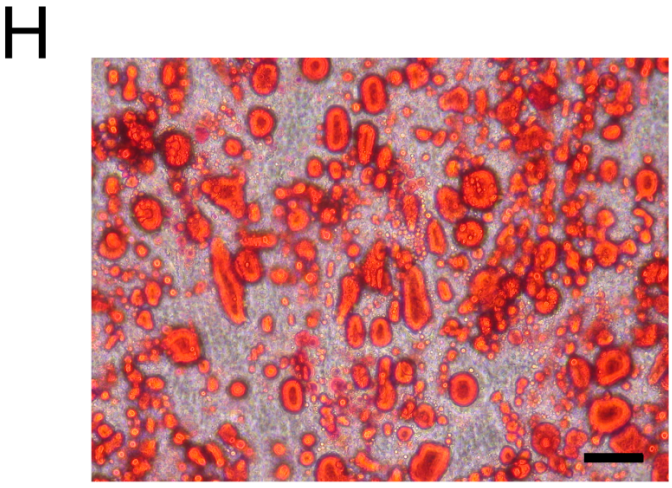
H

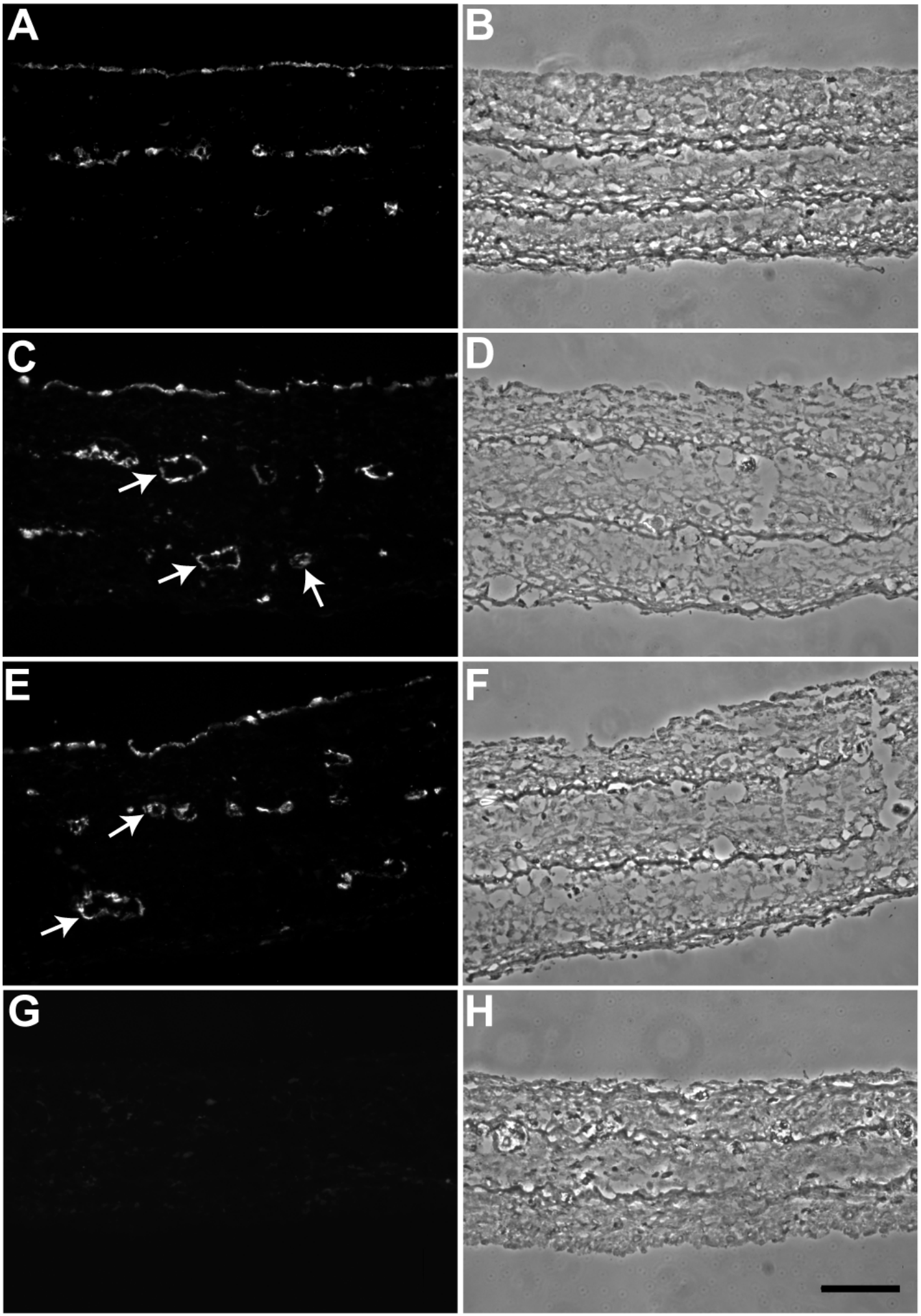
A
B
C
D
E
F
G
H

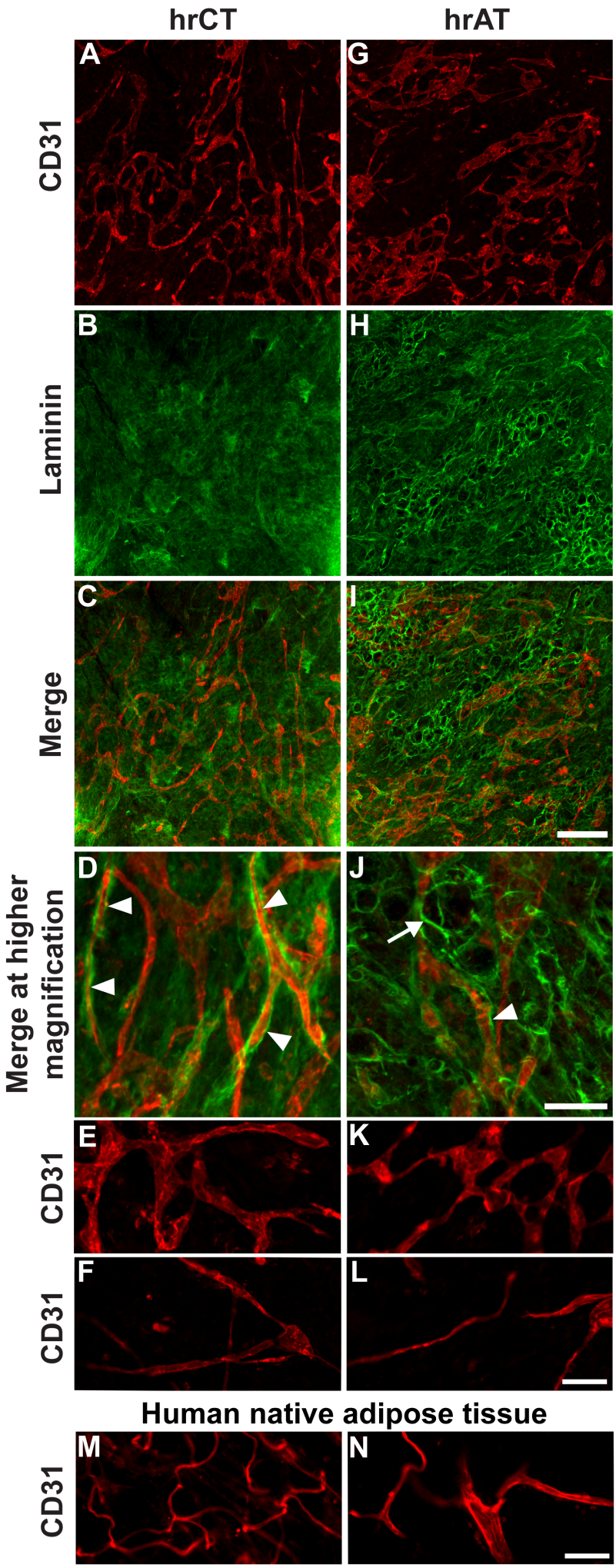
hrCT
hrAT
A
G
CD31
B
H
Laminin
C
I
Merge
D
J
Merge at higher magnification
E
K
CD31
F
L
CD31
Human native adipose tissue
M
N
CD31

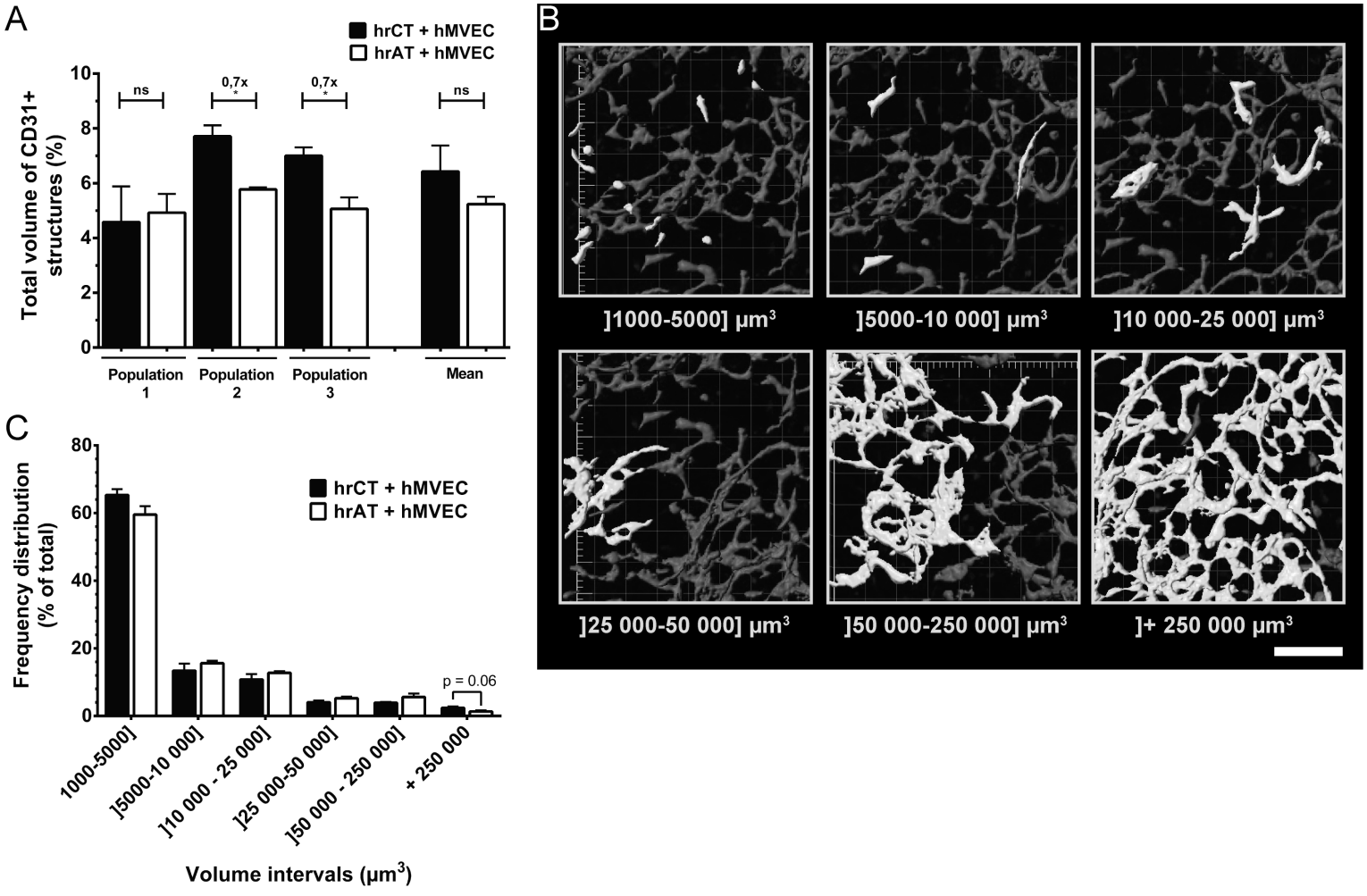
A
hrCT + hMVEC
hrAT + hMVEC
Total volume of CD31+ structures (%)
ns
0,7x
0,7x
ns
Population 1
Population 2
Population 3
Mean
B
]1000-5000] µm³
]5000-10 000] µm³
]10 000-25 000] µm³
]25 000-50 000] µm³
]50 000-250 000] µm³
]+ 250 000 µm³
C
hrCT + hMVEC
hrAT + hMVEC
Frequency distribution (% of total)
p = 0.06
1000-5000]
]5000-10 000]
]10 000 - 25 000]
]25 000-50 000]
]50 000 - 250 000]
+ 250 000
Volume intervals (µm³)

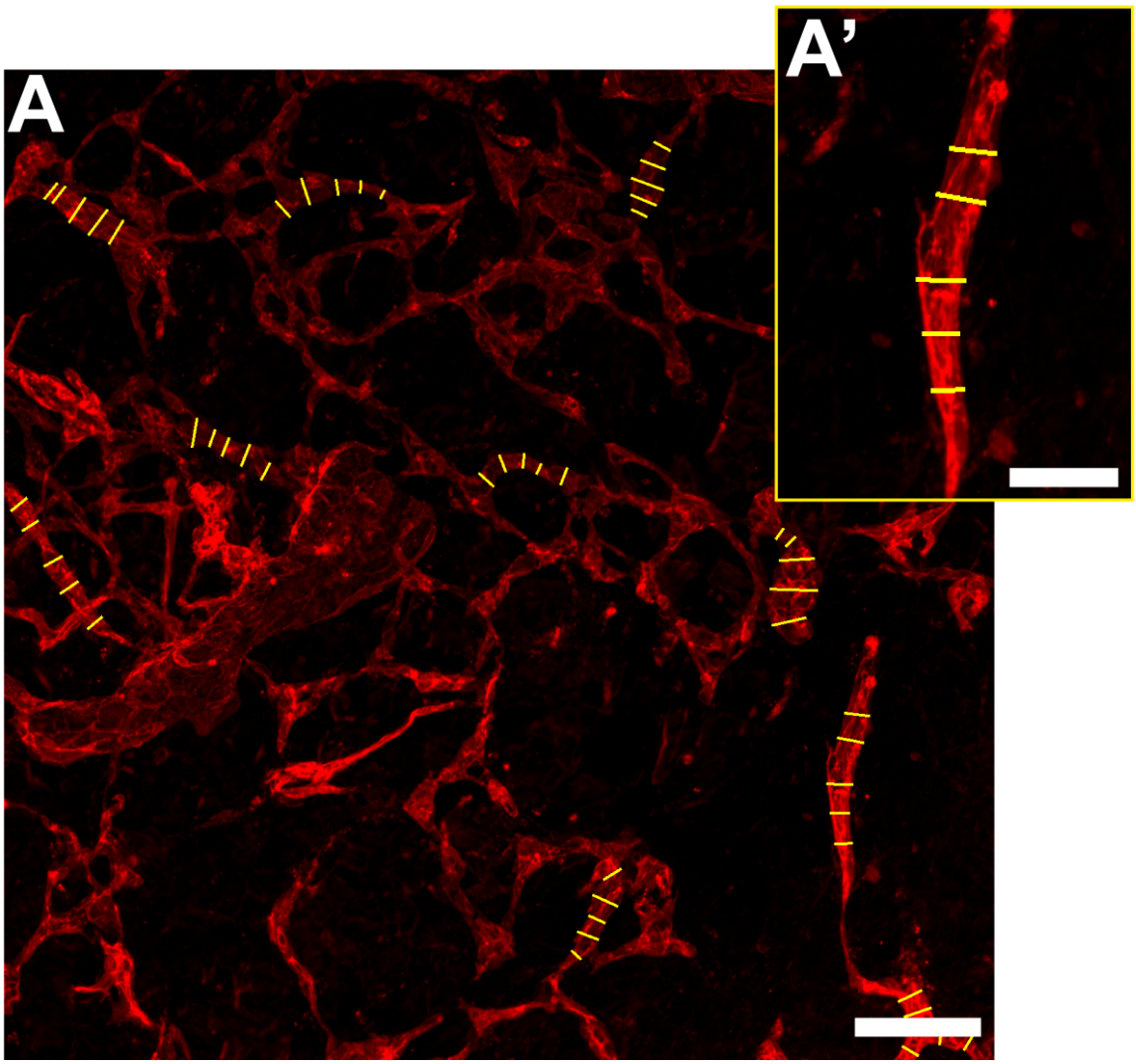
A
A'

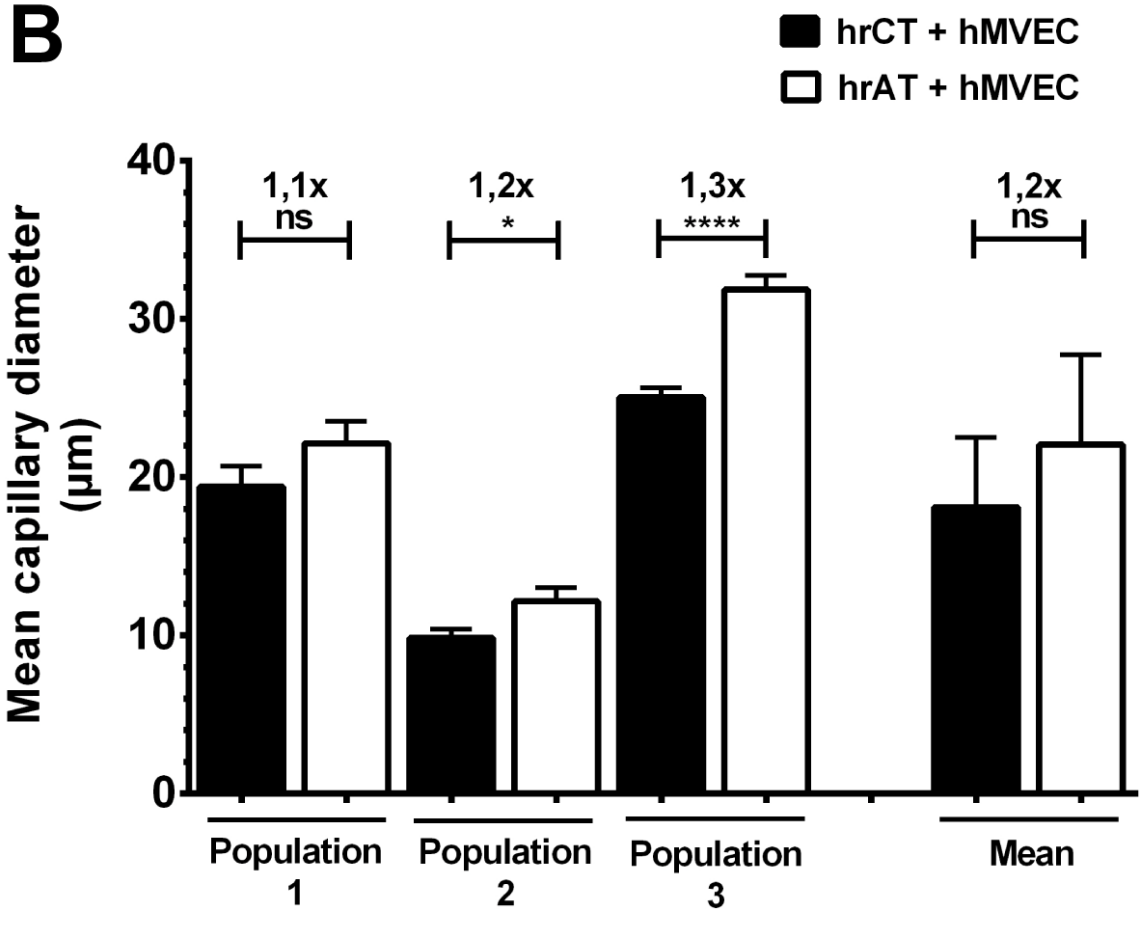
B
hrCT + hMVEC
hrAT + hMVEC
Mean capillary diameter (µm)
40
30
20
10
0
1,1x
ns
1,2x
*
1,3x
****
1,2x
ns
Population 1
Population 2
Population 3
Mean

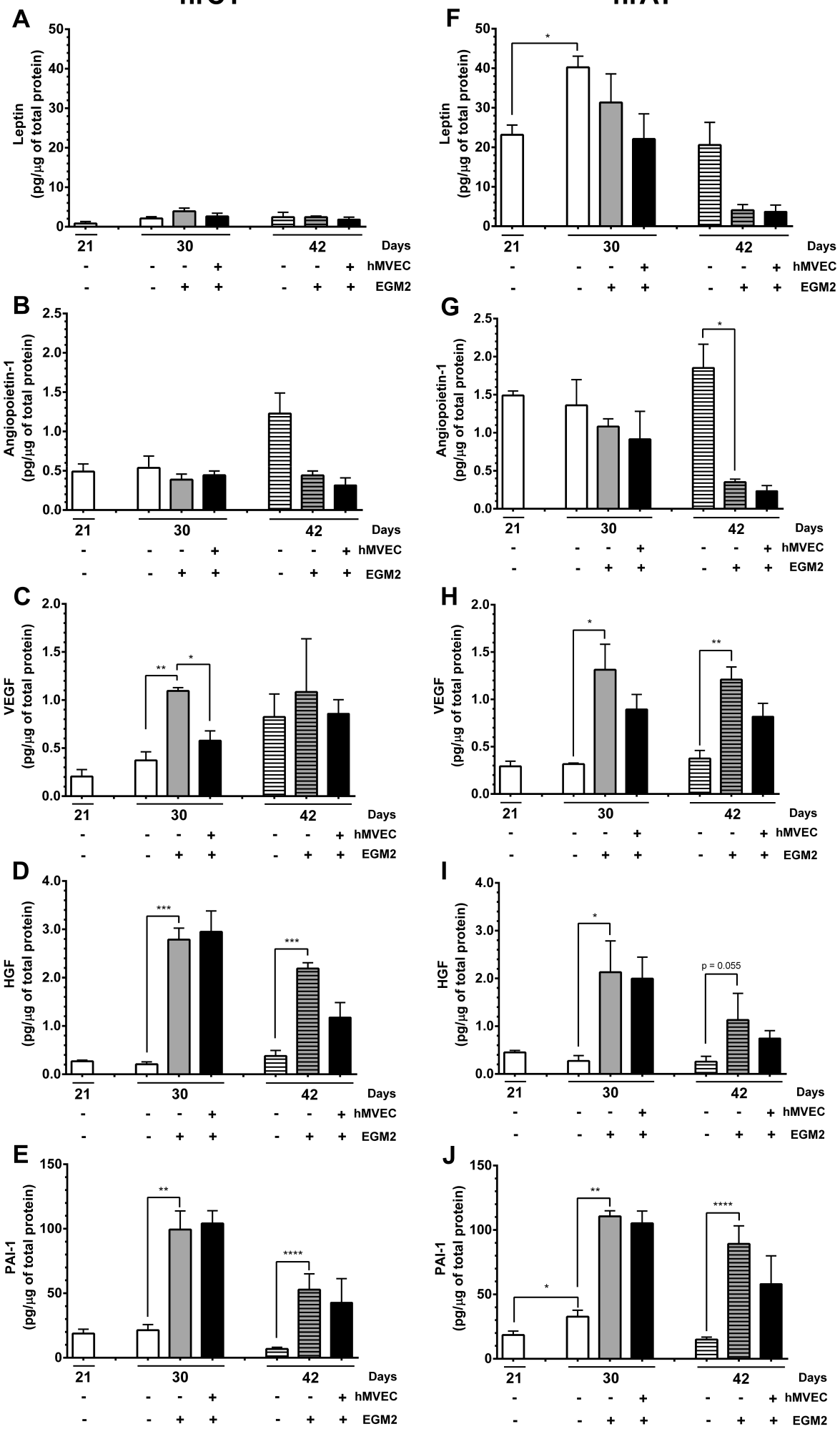
hrCT
hrAT
A
F
Leptin (pg/μg of total protein)
B
G
Angiopoietin-1 (pg/μg of total protein)
C
H
VEGF (pg/μg of total protein)
D
I
HGF (pg/μg of total protein)
E
J
PAI-1 (pg/μg of total protein)
21
30
42
Days
hMVEC
EGM2
p = 0.055

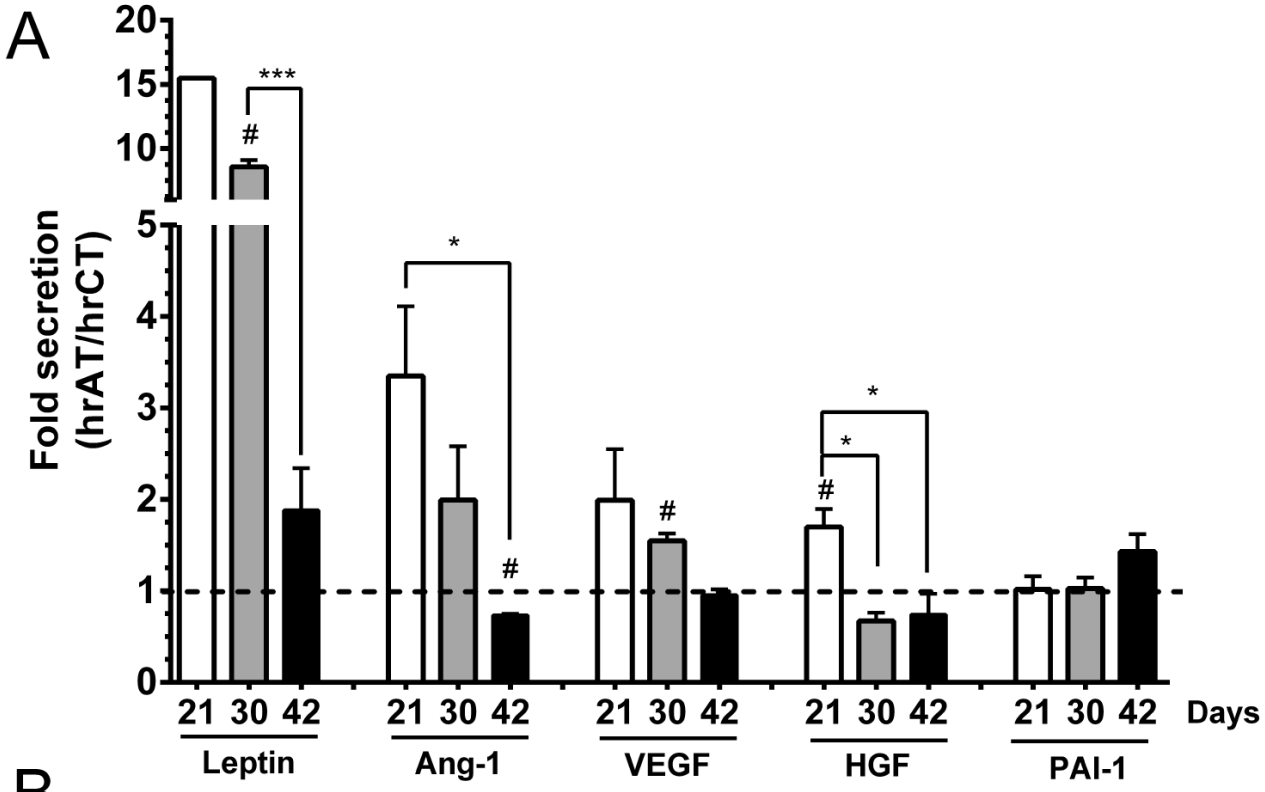
A
Fold secretion (hrAT/hrCT)
20
15
10
5
4
3
2
1
0
***
*
*
*
#
#
#
#
21 30 42
Leptin
Ang-1
VEGF
HGF
PAI-1
Days

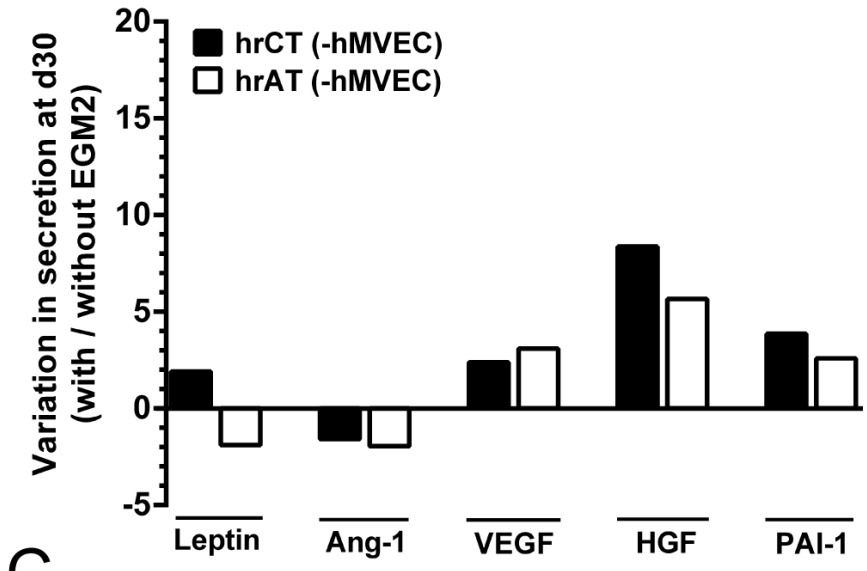
B
Variation in secretion at d30 (with / without EGM2)
hrCT (-hMVEC)
hrAT (-hMVEC)
20
15
10
5
0
-5
Leptin
Ang-1
VEGF
HGF
PAI-1

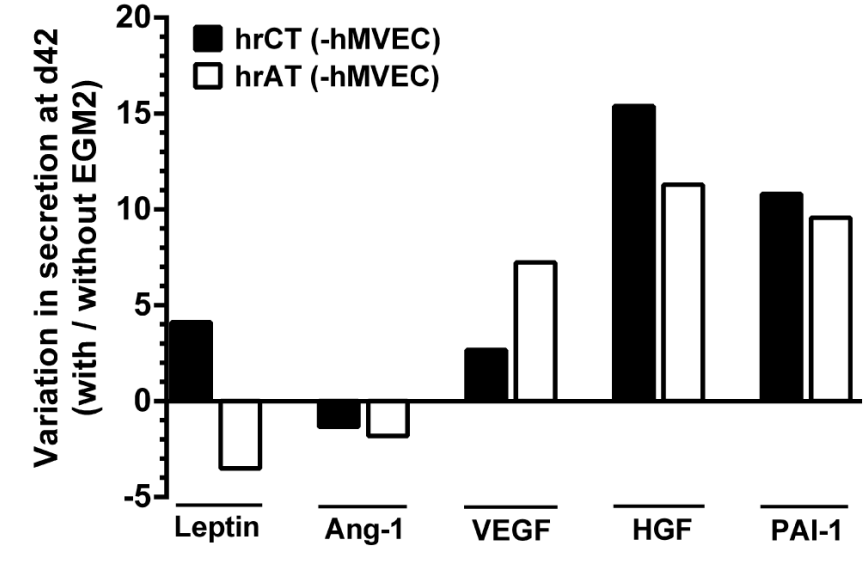
C
Variation in secretion at d42 (with / without EGM2)
hrCT (-hMVEC)
hrAT (-hMVEC)
20
15
10
5
0
-5
Leptin
Ang-1
VEGF
HGF
PAI-1